

The Effect of Intercritical Annealing Temperature on the Structure of Niobium Microalloyed Dual-Phase Steel

MARK D. GEIB, DAVID K. MATLOCK, AND GEORGE KRAUSS

The structures produced in a Nb-microalloyed steel by oil quenching after intercritical anneals at 760 and 810 °C have been examined by light and transmission electron microscopy. After both anneals, the periphery of the austenite pool transforms on cooling to ferrite in the same orientation as the ferrite retained during intercritical annealing. Thus the ferrite forms by an epitaxial growth mechanism without the formation of a new interface or grain boundary. The new ferrite is precipitate-free in contrast to the retained ferrite which develops a very dense precipitate dispersion during intercritical annealing. In the carbon-enriched interior of the austenite pool beyond the epitaxial ferrite only martensite forms in specimens annealed at 760 °C but various mixtures of ferrite and cementite form in specimens annealed at 810 °C. The latter structures include lamellar pearlite, a degenerate pearlite, and cementite interphase precipitation. All Nb is in solution in the austenite formed at 810 °C, and therefore the low hardenability of the specimens annealed at that temperature is best explained by the effect of low austenite carbon content.

INTRODUCTION

AT least some martensite is necessary to produce the high work hardening rate and continuous deformation behavior of dual-phase steels.¹ Cooling rate, intercritical annealing temperature, and alloying all significantly affect the amount of martensite that forms from the austenite produced at the annealing temperature. For example, at high rates of cooling, the austenite transforms predominately to martensite, at intermediate rates to combinations of martensite, acicular ferrite, and ferrite-carbide mixtures, and at low rates to the ferrite and pearlite of conventionally treated mild steels.¹ With respect to alloying, manganese contents around 1.5 pct together with small amounts of vanadium produce sufficient martensite for dual-phase behavior after air cooling from intercritical annealing temperatures.^{2,3} Sufficient alloying even permits the attainment of dual-phase properties directly after hot rolling and coiling⁴ and by box annealing of cold rolled sheet.⁵

In addition to the extent of martensite formation, the amount of proeutectoid ferrite formation around the edges of the austenite pools is also an important aspect of dual-phase microstructure development. Davies³ showed that air cooling a V microalloyed steel from a wide range of temperatures in the austenite-ferrite field resulted in almost identical amounts of martensite, a striking demonstration of the fact that much of the austenite present in the specimens annealed at the higher temperatures must have transformed to ferrite prior to martensite formation. Recently, a special etching technique that differentiates the ferrite which existed during the intercritical hold, "old" or "retained"

ferrite, from that formed during cooling, "new ferrite," has been developed.⁶ Light microscopy appears to show that the new ferrite grows from the retained ferrite without the development of an interface despite its sharp differentiation from the old ferrite in specially etched specimens. In view of the apparent oriented growth of the old ferrite acting as a substrate, the proeutectoid ferrite formed on cooling is believed to grow by a special type of epitaxy,⁷ and therefore, has also been termed epitaxial ferrite.¹

The purpose of this paper is to describe by light and transmission electron microscopy the variations of structure produced by changes in intercritical annealing temperature in a Nb-microalloyed steel. The steel used has been shown to be quite sensitive to the etching technique that differentiates new ferrite from retained ferrite. A major purpose of the transmission electron microscopy performed, therefore, was to establish differences in fine structure that might account for the etching behavior and to verify the epitaxial growth of the ferrite formed on cooling.

EXPERIMENTAL PROCEDURE

The composition in wt pct of the steel examined in this investigation is 0.084 pct C, 1.47 pct Mn, 0.34 pct Si, 0.01 pct N, 0.003 pct V, and 0.053 pct Nb. This steel has the designation HT-12 and has also been studied in other investigations of dual-phase behavior.^{1,6}

The steel was received in the as hot rolled condition as 2.79 mm (0.110 in.) thick sheet. Coupons 25.4 × 9.53 mm (1.00 × 0.375 in.) were sheared from the sheet and surface ground to final thickness of 1.91 mm (0.075 in.)

The heat treatment consisted of intercritical annealing at 810 or 760 °C in neutral salt baths for times ranging from 1 to 64 min followed by quenching to room temperature in still oil.

Heating and cooling curves were obtained by em-

MARK D. GEIB is Graduate Research Assistant, DAVID K. MATLOCK is Professor, and GEORGE KRAUSS is AMAX Foundation Professor, Department of Metallurgical Engineering, Colorado School of Mines, Golden, CO 80401.

Manuscript submitted March 25, 1980.

bedding a 0.508 mm (0.020 in.) Inconel-sheathed, chromel-alumel thermocouple in a coupon welded to a calibration fixture.¹ The thermocouple output was recorded as a function of time with a high speed chart recorder. At each annealing temperature the fixture was immersed in the molten salt, found to reach temperature in 30 to 60 s, and quenched into the oil bath. The chart recorder was left on during the entire procedure so as to record heating as well as cooling curves. Cooling rates were determined at each point, except the first and last, by best fitting a parabola to 3 data points, including the points before and after the point of interest. Maximum cooling rates of 430 and 466 °C/s were measured for samples annealed at 760 and 810 °C respectively.

Thin films for transmission electron microscopy (TEM) were prepared by first removing a slice 2.54 mm (0.10 in.) thick from each coupon from the plane of the sheet with a diamond saw. The slices were chemically thinned with a HF-H₂O₂ solution to a thickness of 0.025 to 0.076 mm (0.001 to 0.003 in.). Then 3 mm (0.12 in.) diam discs were removed and demagnetized. The discs were jet polished in a Cr₂O₃-glacial acetic acid solution and examined in a Philips 400 EM fitted with a tilting goniometer stage. All specimens were examined with an accelerating voltage of 120 KV.

The etching technique used to differentiate old and new ferrite consists of etching in picral followed by immersion in a boiling alkaline chromate solution. Full details of the etching procedure are given elsewhere.⁶

RESULTS AND DISCUSSION

A. Light Microscope Observations

Figures 1(a) and (b) show the optical microstructures of the Nb-microalloyed steel after oil quenching from 760 and 810 °C respectively. The letters on each micrograph indicate types of areas that were also characterized by TEM as summarized in the following section. In each microstructure the alkaline chromate etch has stained or darkened the old or retained ferrite gray. The boundaries between the gray and white areas delineate the extent of the austenite pools formed during holding at the intercritical annealing temperature.⁶

Within the white patches darker etching structures are present. In the specimen annealed at 760 °C the interior structures etch a uniform black, and as identified by TEM, consist almost entirely of martensite not resolvable in the light microscope. In the specimen annealed at 810 °C the interior of the prior austenite pools show a much greater variation in structure and etching response. Parallel lamellae are readily visible at the edges of the white ferrite rim. The interlamellar spacing decreases somewhat and then the lamellar structure gives way to a gray-etching structure not resolvable in the light microscope. Some black areas corresponding to martensite are also visible in the prior austenite pools but their area fraction in the microstructure is considerably less than the black martensitic areas of the specimens annealed at 760 °C.

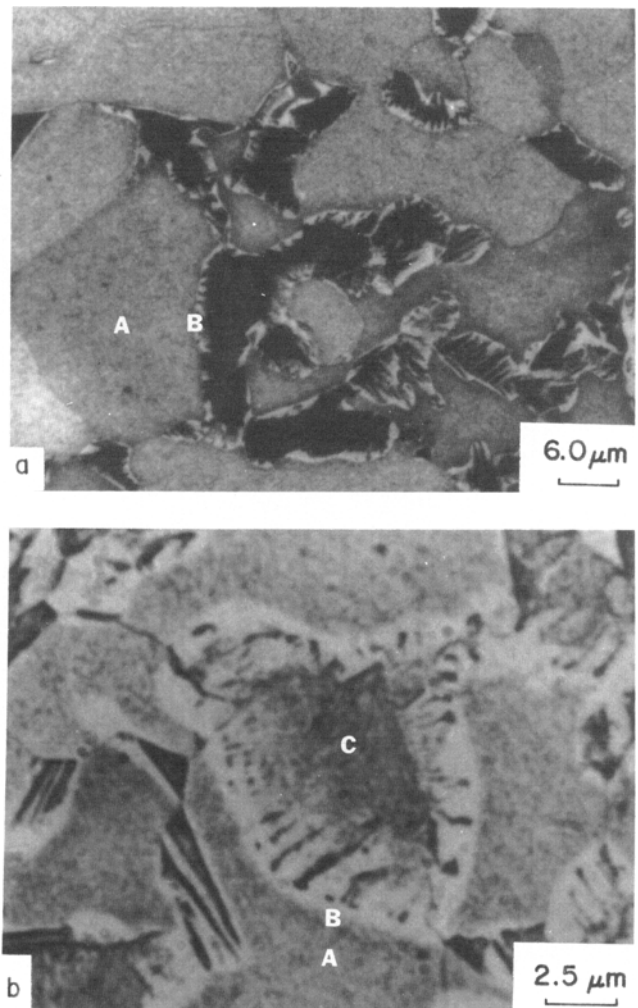


Fig. 1—Microstructures of Nb-microalloyed steel annealed at (a) 760 °C for 8 min and (b) 810 °C for 16 min. Letters identify areas examined by TEM. Boiling alkaline chromate etch, light micrographs.

The above observations show that much more martensite forms after annealing at 760 than at 810 °C. Thus, the hardenability of the austenite formed by intercritical annealing at 760 °C is significantly higher than that of the austenite formed at 810 °C. Perhaps the most ready explanation of the hardenability difference is the higher carbon content of the austenite formed at 760 °C and the well known effect of carbon on the hardenability of steels.^{8,9} However, the niobium addition may also affect hardenability. Eldis and Hagel¹⁰ showed that Nb in low carbon, 1.47 pct Mn steels could either enhance hardenability if in solution in the austenite or could detract from hardenability if austenizing was performed at the relatively low temperature of 925 °C where presumably niobium carbonitride precipitation occurs. Thus, the differences in hardenability noted between the 760 and 810 °C specimens might be caused in part by carbon variations and in part by the extent of niobium carbonitride precipitation or solution in the austenite pool. Observations concerning the extent of such carbonitride precipitation during intercritical annealing will be discussed in a later section.

B. Transmission Electron Microscopy

At the intercritical annealing temperature only austenite and ferrite are assumed to exist in a low carbon steel. Any cementite present in the as-rolled microstructure has combined with ferrite and produced austenite provided sufficient time has elapsed. An earlier metallographic study of the niobium microalloyed steel considered here showed that equilibrium amounts of 23 and 47 pct austenite were formed in about 5 min at 760 and 810 °C respectively.⁶ This section first describes the fine structure of the majority phase, the old ferrite or ferrite retained during intercritical annealing. Retained ferrite areas are identified by the letter A in Fig. 1. Then structures produced by the transformation of austenite during oil quenching from the intercritical annealing temperature are discussed. Transformation products close to the ferrite-austenite interfaces, areas identified by the letter B in Fig. 1, and unique ferrite-cementite structures, from areas similar to that marked C in Fig. 1(b), are also described.

1. The Structure of Retained Ferrite. Figure 2 shows the changes that develop in the fine structure of the ferrite in the as-rolled Nb-microalloyed steel as a result of intercritical annealing. Micrographs of as-rolled ferrite and ferrite annealed at 760 and 810 °C are shown.

The as-rolled ferrite contained a relatively low dislocation density, Fig. 2(a). The dislocations present were frequently pinned, apparently by a dispersion of fine particles. The particles were 20 nm or smaller in size. Several of the larger particles are identified by arrows in Fig. 2(a). In view of the composition of the steel and the identification of similar particles in similar steels,¹¹⁻¹³ the particles are most probably niobium carbonitrides.

The relatively large size and spacing of the particles are consistent with a general precipitation within recrystallized austenite during hot working.¹⁴ A number of observations support this statement. The steel was not controlled rolled, and therefore, the relatively coarse ferrite grain size, 20 μm, developed from a coarser equiaxed austenite grain structure. Controlled rolled steels finished at low temperatures generally have much finer ferrite grain sizes, 5 μm or less^{14,15} as a result of ferrite formation in the deformed austenite. In microalloyed steels that are controlled rolled the niobium carbonitrides precipitate out on the deformation substructure of the austenite and produce particle arrays much different from that shown in Fig. 2(a).^{11,12,15} Precipitation during the austenite to ferrite transformation after hot rolling would also have produced a distribution of carbonitride particles much different from that observed. Such precipitation is referred to as interphase precipitation and produces rows or sheets or particles in the ferrite.^{11,16,17}

Figure 2(b) shows the fine structure of ferrite retained throughout an intercritical anneal at 760 °C. Large (20 nm), widely dispersed particles are still present, but a dispersion of very fine particles, 2 nm or less in diam has also developed. The fine particle dispersions appear to be a result primarily of a general matrix precipitation. Most of the dislocations are free of precipitate particles,

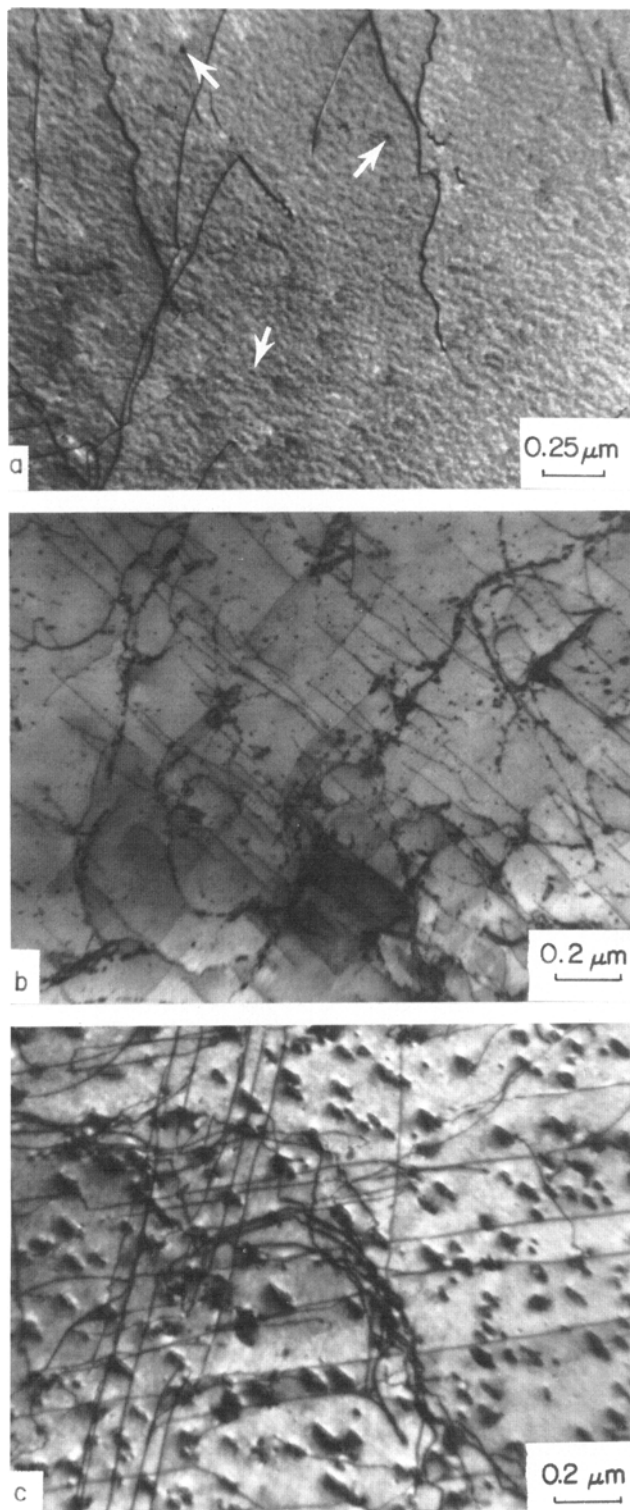


Fig. 2—Examples of fine structure in retained ferrite of specimens (a) as-rolled, (b) annealed at 760 °C for 8 min, (c) annealed at 810 °C for 8 min. Areas in (b) and (c) correspond to areas marked A in Fig. 1. TEM micrographs.

probably because the dislocations formed during cooling only after the precipitates had formed at the intercritical annealing temperature. Some of the precipitate particles are aligned in linear arrays, and may have preferentially precipitated on the dislocations

initially present in the hot rolled structure, Fig. 2(a).

The area shown in Fig. 2(b) was centrally located in a retained ferrite grain and removed from areas that were austenitic during annealing. Nevertheless, the dislocation density is high and an incipient cell structure has developed.

Figure 2(c) shows the fine structure of ferrite retained during intercritical annealing at 810 °C. Figure 2(c) was taken at the same magnification as Fig. 2(b) and therefore shows that a much coarser carbonitride distribution develops as a result of the higher temperature anneal. The actual size of the particles cannot be accurately estimated because of the inability to separate the strain fields from the particles in our micrographs. Examples of coherency strain fields associated with plate-shaped carbonitrides precipitated in ferrite have been presented in the literature.^{11,12,17} However, Fig. 4 shows a pyramidal or triangular precipitate morphology in the interface area of retained ferrite and transformed austenite. Strain fields on one side of each triangular particle are in good contrast. It is possible that the triangular precipitates and some of the other precipi-

tates in the retained ferrite are in fact phases other than niobium carbonitrides. In view of the high nitrogen content of the Nb-microalloyed steel some of the precipitates may in fact be aluminum nitrides.^{18,19} The complete characterization of the precipitate particle distributions was outside of the scope of the present survey of structures and needs more intensive future investigation.

The series of micrographs in Fig. 2 clearly shows that intercritical annealing produces well developed precipitate distributions in ferrite retained during intercritical annealing at 760 and 810 °C. This result is consistent with the findings of Hoogendoorn and Spanraft.¹³ They found in V and Nb microalloyed steels that substantial precipitation of carbonitrides on heating began just below the lower critical temperature at temperatures between 650 and 700 °C. The amount of precipitation was also dependent on the amount already precipitated during rolling. The latter factor helps to explain the well developed precipitate distributions in Figs. 2(b) and (c). In view of the relatively small amount of precipitation in the as-rolled ferrite, Fig. 2(a), the supersaturation of the ferrite prior to intercritical annealing must have been quite high.

2. Transformation-Induced Dislocation Substructure.

Figure 3 compares the dislocation structure produced in specimens intercritically annealed at 760 and 810 °C. Figure 3(a) shows a very high dislocation density in ferrite adjacent to martensite that has formed on quenching from 760 °C. The dislocations are concentrated in tangles that define cells or dislocation-free areas. Figure 3(b) shows a much lower dislocation density in the ferrite adjacent to an area that has transformed to a ferrite-cementite mixture on oil quenching from 810 °C. Semicircular loops at the interface of the transformation zone give way to arrays of long, straight dislocations in areas removed from the interface. Hornbogen¹⁸ has characterized such arrays in an Fe-0.9 pct Cu alloy and attributed their formation to the increased mobility of edge dislocations relative to

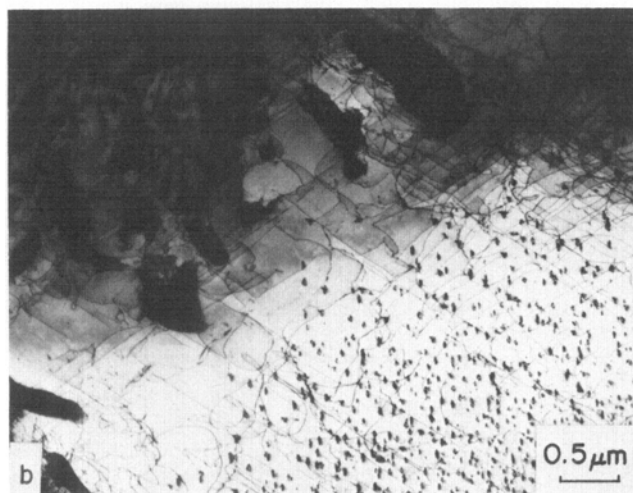
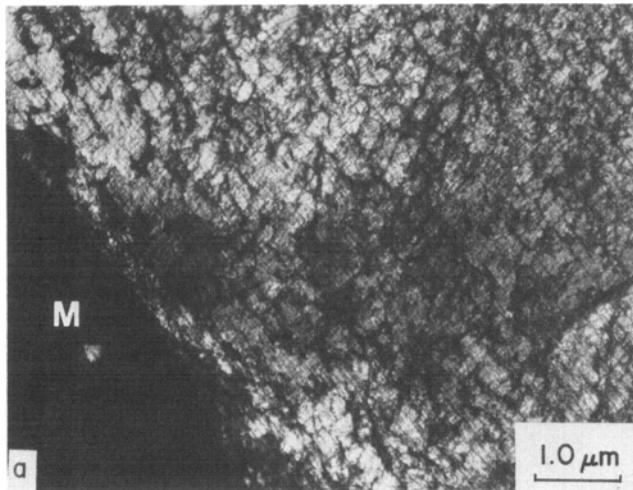


Fig. 3—Examples of dislocation substructure adjacent to transformed austenite in specimens annealed at (a) 760 °C for 8 min, and (b) 810 °C for 8 min. Areas shown correspond to areas marked B on Fig. 1. TEM micrographs.

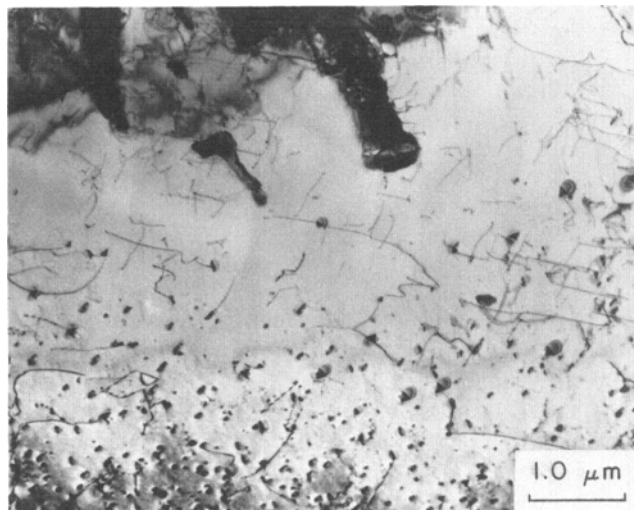


Fig. 4—Precipitate-free zone between retained ferrite and ferrite-cementite austenite transformation product in a specimen annealed at 810 °C for 8 min. TEM micrographs.

that of screw dislocations in a dispersion of Cu precipitate particles in ferrite.

The micrographs of Fig. 3 show that the mechanisms of austenite transformation profoundly influence the nature of the dislocation substructure in the ferrite of intercritically annealed steels. Diffusion-controlled transformation with its atom by atom formation of the product phases results in a much lower dislocation density than does shear transformation to martensite. The effects of the various dislocation substructures and their distribution within the retained ferrite on work hardening of dual-phase steels have been discussed elsewhere.¹

3. Austenite Transformation Products. This section describes unique products of austenite transformation in intercritically annealed steels. In particular the initial transformation to ferrite and several nontypical eutectoid structures are described.

Figure 4 shows a region where austenite at the periphery of the pool has transformed to ferrite. As a result carbon has been rejected to the interior of the pool which transforms to a pearlitic structure of cementite and ferrite during quenching from 810 °C. Several cementite lamellae are visible in the upper part of the micrograph. Some retained ferrite with a uniform distribution of carbonitride particles similar to those shown in Fig. 2(c) and Fig. 3(b) is also included in the field of view. The amount of precipitation decreases as the transformation products of the prior austenite pool are approached. The decrease in particle density to a negligible quantity marks the interface between the ferrite and austenite at the intercritical annealing temperature. Although not quite as sharply defined as in the light micrograph, Fig. 1(b), the 1 to 2 μm width of the precipitate-free zone between the retained ferrite and the pearlite agrees with the widths of the white zones in the light micrographs.

The observation of the precipitate-free ferrite zone adjacent to the precipitated retained ferrite establishes several important characteristics of the intercritical annealing process. First, the austenite that forms on intercritical annealing dissolves any carbonitride precipitates initially present. Therefore, the austenite has significantly higher solubility for the Nb carbonitrides than does ferrite. Second, the carbonitrides do not reprecipitate in the new ferrite on cooling. Third, there is no structural interface, subboundary, or grain boundary between the new ferrite and retained ferrite. The new ferrite forms directly by growth on the existing retained ferrite, without the need to nucleate a new crystal orientation. This process, therefore, may certainly be considered to be a special type of epitaxial growth and thus, the TEM evidence supports the earlier light microscope observations of epitaxy.^{1,6} A similar conclusion of the reversible migration of austenite/ferrite interfaces has recently been made after study of austenite formation in an Fe-1V-0.2C steel.²⁰ In the latter study, however, solution and reprecipitation of vanadium carbide in the austenite was observed. Finally, the differences in etching response between new ferrite and retained ferrite may be directly related to differences in fine structure between the two forms of ferrite. Either a surface roughening due to the precip-

itates in the retained ferrite and/or the changed chemistry of the ferrite matrix where precipitation has occurred could contribute to the differential etching response of the two ferrites.

Figure 5 compares the pearlite of the as-hot rolled Nb

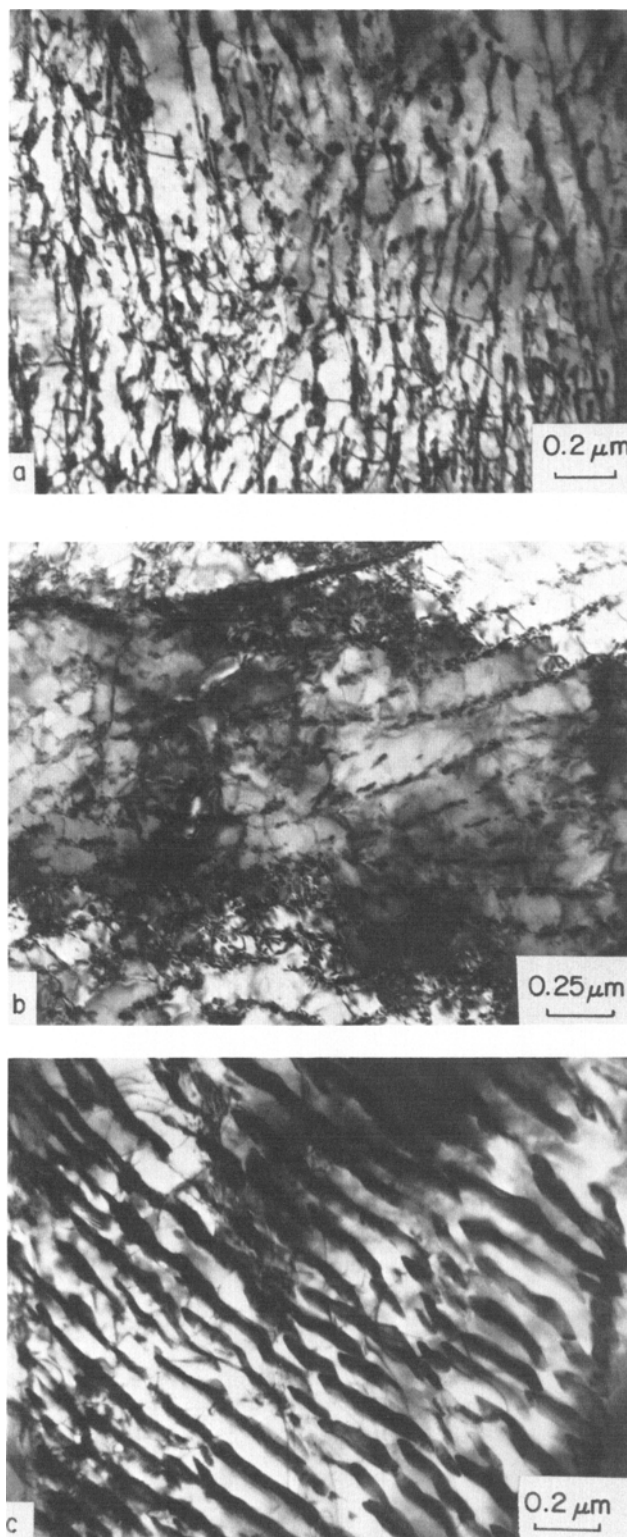


Fig. 5—Various types of eutectoid structures in Nb microalloyed steel. (a) Degenerate pearlite in specimen annealed at 810 °C for 32 min, (b) interphase precipitation in specimen annealed at 810 °C for 16 min and (c) pearlite in an as-rolled specimen. Areas (a) and (b) correspond to area marked C in Fig. 1. TEM micrographs.

steel to modifications of eutectoid structure that formed during oil quenching from an intercritical annealing temperature of 810 °C. The modified eutectoid structures were not formed in specimens intercritically annealed at 760 °C. In the latter specimens the austenite transformed almost completely to martensite. The only evidence of diffusion-controlled transformation was a thin zone of new ferrite between the retained ferrite and martensite patches.

Figure 5(a) shows a degenerate eutectoid morphology that formed in the center of a pool of austenite after intercritical annealing at 810 °C. The carbide particles are aligned in a direction roughly normal to the transformation interface (as shown by low magnification observations), but have not developed in a continuous, lamellar morphology. Figure 5(b) shows an example of row or interphase precipitation where the carbide particles align themselves parallel to the transformation interface. Selected area diffraction showed that the particles in all of the eutectoid structures were cementite. The two types of eutectoid structures formed on quenching from 810 °C should be compared to the more typical pearlite structure of the as-rolled steel, Fig. 5(c).

Interphase precipitation has been observed most frequently in steels containing strong carbide forming elements such as Cr, Mo, Ti, Nb, V, and W^{16,21} that form alloy carbides at the austenite-ferrite interface on transformation. More recently, interphase precipitation of cementite in a continuously cooled plain carbon steel has been documented.²¹ Nevertheless it is surprising to find interphase precipitation of cementite in the Nb steel, especially in view of the frequent observation of Nb carbonitride row precipitation in Nb-containing steels.^{11,16,22} The reason for this finding is presented in the work of Gray and Yeo.²² They found that row precipitation of Nb carbonitride particles occurs only if a critical cooling rate is not exceeded. In specimens cooled at a rate faster than the critical, cementite, usually in the form of pearlite rather than an alloy

carbide, formed. At high cooling rates the diffusion of Nb necessary for the nucleation and growth of Nb carbonitrides is suppressed. Thus, on the basis of a kinetic argument, the cooling of specimens of the Nb microalloyed steel oil quenched from 810 °C apparently exceeded the critical rate not only for Nb carbonitride formation but also for normal pearlite formation in the center of the austenite pools. Figure 6, taken from Gray and Yeo, shows a schematic CCT diagram that accounts for the cementite formation during cooling at rates above the critical rate for NbC (N) formation.

A final point of discussion is the effect of Nb on hardenability. It has now been demonstrated, as shown in Fig. 4, that Nb is almost completely dissolved in austenite formed during intercritical annealing at 810 °C. Nevertheless, the hardenability of austenite formed at 810 °C is much lower than that formed at 760 °C. Thus, the effect of the higher austenite carbon content at the lower temperature must be the major factor contributing to the enhanced hardenability produced by low temperature annealing. Although the positive effect of carbon on hardenability is experimentally well known,^{8,9} the mechanisms of enhancement are not clear at this time. Perhaps the significantly higher carbon gradients developed ahead of the epitaxial ferrite transformation front at 810 °C enhance the rate of pearlite formation.

CONCLUSIONS

1. Intercritical annealing produces precipitation in the retained ferrite of a Nb-microalloyed steel. The precipitates are assumed to be Nb carbonitrides but other phases such as Al nitride may also precipitate. The precipitate dispersion coarsens with increasing intercritical annealing temperature.
2. On cooling from the intercritical annealing temperature the periphery of the austenite pool transforms to ferrite by an epitaxial growth mechanism. No precipitation occurs in this new ferrite.

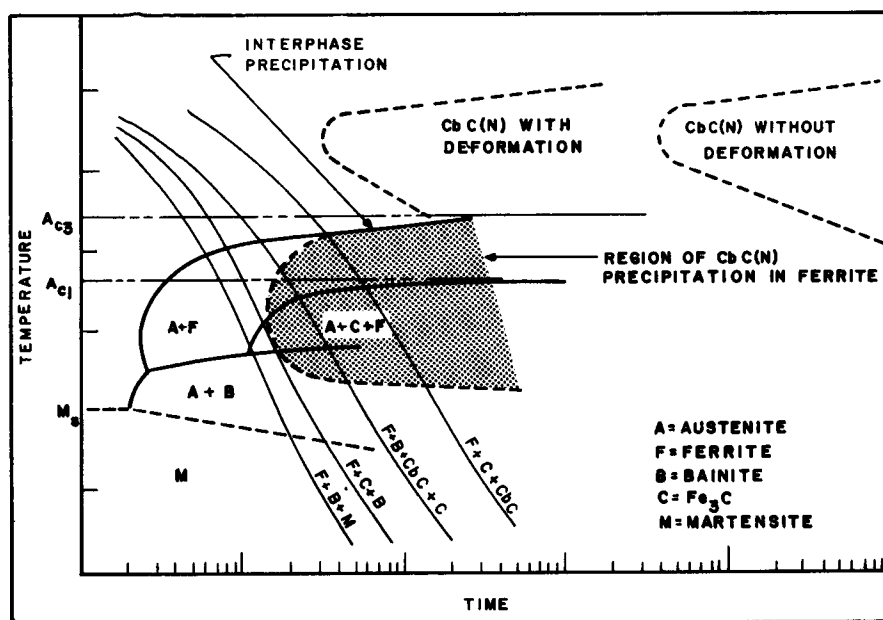


Fig. 6—Schematic CCT diagram for Nb microalloyed steel. After Gray and Yeo.²²

3. The discontinuity in precipitation at the interface of the new and retained ferrite provides an explanation for the differentiation of the two forms of ferrite by etching.

4. The hardenability of the austenite formed by intercritical annealing decreases with increasing annealing temperature. The increased hardenability is apparently due to the higher carbon content of austenite formed at lower temperatures and is not due to the Nb in solution in the austenite.

5. Austenite transforms to special eutectoid structures consisting of degenerate pearlite and cementite inter-phase precipitation after epitaxial ferrite and lamellar pearlite have formed in specimens oil quenched from 810 °C. Only martensite forms in the carbon-enriched austenite beyond the epitaxial ferrite of specimens oil quenched from 760 °C.

6. The transformation of austenite by diffusion-controlled mechanisms in specimens quenched from 810 °C produces a much lower dislocation density in the retained ferrite than does shear transformation to martensite in specimens quenched from 760 °C.

ACKNOWLEDGMENTS

The authors acknowledge the support of the AISI and the AMAX Foundation for this work. The experimental assistance of Richard Lawson, research assistant at the Colorado School of Mines, is deeply appreciated.

REFERENCES

1. David K. Matlock, George Krauss, Luis F. Ramos, and Glenn S. Huppi: *Structure and Properties of Dual-Phase Steels*, R. A. Kot and J. W. Morris, eds., pp. 62–90, TMS-AIME, Warrendale, PA, 1979.
2. M. S. Rashid: Automotive Engineering Congress, Rep. No. 760206, Detroit, Soc. Auto. Engineers, 1976.
3. R. G. Davies: *Met. Trans. A*, 1978, vol. 9A, pp. 41–52.
4. A. P. Coldren, G. Tither, A. Cronford, and J. R. Hiam: *Formable HSLA and Dual-Phase Steels*, A. T. Davenport, ed., pp. 205–26, TMS-AIME, Warrendale, PA, 1979.
5. P. R. Mould and C. C. Skena: *Formable HSLA and Dual-Phase Steels*, A. T. Davenport, ed., pp. 181–204, TMS-AIME, Warrendale, PA, 1979.
6. Richard D. Lawson, David K. Matlock, and George Krauss: *Metallography*, 1980, vol. 13, pp. 71–87.
7. I. H. Khan: *Handbook of Thin Film Technology*, L. I. Maissel and R. Giang, eds., pp. 10–13, McGraw-Hill, Inc., New York, 1970.
8. M. A. Grossman and E. C. Bain: *Principals of Heat Treatment*, 5th ed., ASM, Metals Park, OH, 1964.
9. C. A. Siebert, D. V. Doane, and D. H. Breen: *The Hardenability of Steels*, ASM, Metals Park, OH, 1977.
10. G. T. Eldis and W. C. Hagel: *Hardenability Concepts with Applications to Steel*, D. V. Doane and J. S. Kirkaldy, eds., pp. 397–413, AIME, Warrendale, PA, 1978.
11. A. T. Davenport, L. C. Brossard, and R. E. Miner: *J. Met.*, June 1975, vol. 27, pp. 21–7.
12. P. L. Mangonon, Jr. and W. E. Heitmann: *Microalloying '75*, pp. 59–74, Union Carbide Corporation, New York, 1977.
13. T. M. Hagendoorn and M. J. Spanraft: *Microalloying '75*, pp. 75–85, Union Carbide Corporation, New York, 1977.
14. J. M. Gray: *Processing and Properties of Low-Carbon Steel*, J. M. Gray, ed., pp. 225–42, AIME, Warrendale, PA, 1973.
15. M. Cohen and S. S. Hansen: ASTM STP 672, pp. 34–52, American Society for Testing and Materials, Philadelphia, PA, 1979.
16. R. W. K. Honeycombe: *Met. Trans. A*, 1976, vol. 7A, pp. 915–36.
17. L. Meyer, F. Heisterkamp, and W. Mueshenborn: *Microalloying '75*, pp. 153–67, Union Carbide Corporation, New York, 1977.
18. E. L. Brown, A. J. DeArdo, and J. H. Bucher: *The Hot Deformation of Austenite*, pp. 250–85, AIME, 1977.
19. T. Sakai, M. Shiozaki, and K. Takashina: *J. Appl. Phys.*, 1979, vol. 50, pp. 2369–71.
20. N. C. Law and D. V. Edmonds: *Met. Trans. A*, 1980, vol. 11A, pp. 33–46.
21. A. T. Davenport and P. C. Becker: *Met. Trans.*, 1971, vol. 2, pp. 2962–64.
22. J. M. Gray and R. B. G. Yeo: *ASM Trans. Q.*, 1968, vol. 61, pp. 255–69.